International Journal of Energy and Power Engineering
2024, Vol. 13, No. 4, pp. 67-72
https://doi.org/10.11648/j.ijepe.20241304.12

Research Article

Improvements in Transient Testing Reactor (TREAT) with a Choice of Filter

Harish Aryal*

Mechanical Engineering, Marymount University, Arlington, The United States

Abstract

The safe and reliable operation of nuclear reactors has always been one of the topmost priorities in the nuclear industry. Transient testing allows us to understand the time-dependent behavior of the neutron population in response to either a planned change in the reactor conditions or unplanned circumstances. These unforeseen conditions might occur due to sudden reactivity insertions, feedback, power excursions, instabilities, and accidents. To study such behavior, we need transient testing, which is like car crash testing to estimate the durability and strength of a car design. In nuclear designs, such transient testing can simulate a wide range of accidents due to sudden reactivity insertions and helps study the feasibility and integrity of the fuel used in certain reactor types. This testing involves a high neutron flux environment and real-time imaging technology with advanced instrumentation with appropriate accuracy and resolution to study the fuel slumping behavior. With the aid of transient testing and adequate imaging tools, it is possible to test the safety basis for reactor and fuel designs that serves as a gateway in licensing advanced reactors in the future. To that end, it is crucial to fully understand advanced imaging techniques both analytically and via simulations. This paper presents an innovative method of supporting real-time imaging of fuel pins and other structures during transient testing. The major fuel-motion detection device that is studied in this dissertation is the Hodoscope which requires collimators. This paper provides 1) an MCNP model and simulation of a TREAT core with a central fuel element replaced by a slotted fuel element that provides an open path between test samples and a hodoscope detector, and 2) a choice of good filter to improve image resolution.

Keywords

Hodoscope, Transient Testing, Collimators, MCNP, TREAT, Hodogram, Filters

1. Introduction

1.1. Background

The project provided some advanced instrumentation studies in support of the Transient Reactor Test (TREAT) facility, which is the principal facility in the US for the safety testing of reactor fuel. It was in operation from 1959 to 1994 and has since re-started after a 20-year hiatus. The TREAT restart effort was completed in February 2018, which was one year ahead of schedule and $20 million under budget [19]. It is a high flux, air-cooled, thermal, pulsed reactor. A key instrument used in TREAT is the hodoscope. It records the motion of fissionable material in the test capsule as the fuel fails during accident scenarios. It consists of multi-channel front and back collimators. During the experiment, fast neu-

*Corresponding author: haryal@marymount.edu (Harish Aryal)

Received: 22 May 2023; **Accepted:** 7 June 2023; **Published:** 29 September 2024

trons produced in the test capsule are collimated providing a 2-dimensional “map” of fuel location, and are time stamped in the hodoscope detection system. Hodoscope system measurements need improvements to yield higher-resolution images [2]. Cody uses a cloud chamber to provide useful information that a diffusion cloud chamber based on the temperature differential is better suited than the traditional pulsed one and even if the pulsed one were to be used; mechanical piston movement is preferable to the pneumatic type. This is because the mechanical cloud chambers have variable stopping positions to adjust the desired expansion ratio and are relatively fast. Another advantage of mechanical pistons is that they do not require threshold pressure to move the piston, while the pneumatic chambers have some resetting time before the piston can overcome the friction [1].

“The Principles of Cloud-Chamber Technique” by J. G. Wilson was used to understand the super-saturation, condensation, and growth of drops during cloud formation [3]. Vomer and Flood showed the relationship between the critical super-saturation, the bulk value of surface tension, and molecular mass [Flood]. However, research shows that the cloud chamber is not a viable option even if it might have several advantages (e.g., being able to eliminate the collimator) for TREAT imaging. A diffusion cloud chamber is recommended to be used instead of a pulsed one. It allows an observer to “see” radiation because a trail of condensation is formed in the wake of the particle [20]. Other notable references used for the preparation of this paper are “Experimental Results and Improvements in the Fast Neutron Hodoscope” by De Volpi and C. H Freese [7]; “High Power Level Transient Reactor Test (TREAT) Facility Sodium Loop Meltdown Experiment on an Unbonded EBR-II Mark I Fuel Pin” by E. Dickerman et al [8]; “Fast Neutron Hodoscope at TREAT: Methods for Quantitative Determination of Fuel Dispersal” by A. De. Volpi et al [9]. With an understanding of the significance of transient testing to ensure safety in nuclear reactors, it is inevitable that proper real-time imaging tools be implemented, and this research provides a unique method of creating real-time images during fuel slumping behavior with the right choice of filter.

1.2. Reactor Description

Transient Reactor Test (TREAT) reactor is the principal facility in the US for safety testing of reactor fuel. It was in operation from 1959 to 1994 and has been restarted in 2017 after a 25-year hiatus. It is a high flux, air-cooled, thermal, pulsed reactor. TREAT was designed by Argonne National Laboratory (ANL) and is in INL. The reactor core has a 19 by 19 array of fuel and reflector assemblies, which are 10 cm (4 in) square and 2.7 m (8.8 ft) long. The assemblies contain a 1.2-m (4 ft) active fuel region with 0.6-m (2 ft) reflector regions above and below [13]. The fuel used in TREAT is a mixture of highly enriched UO_2 dispersed in graphite. The graphite has sufficient heat capacity to allow the fuel to reach high temperature during a pulse transient that a strong negative temperature coefficient of reactivity will terminate the pulse. Shielding blocks provide necessary biological shielding. The maximum-allowed core energy and peak power are approximately 2.5 GJ and 19 GW, respectively [13]. A key instrument used in TREAT is the Hodoscope It can record the motion of fissionable material in the test capsule as the fuel fails during accident scenarios. Figures 1 and 2 show the schematics of the TREAT facility and the hodoscope (plan and elevation views) respectively.

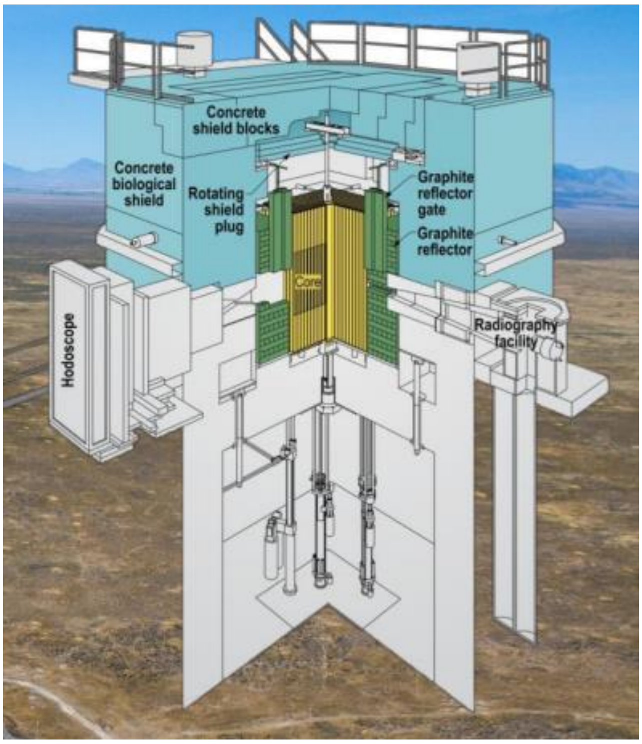

Figure 1. *Sketch of TREAT with Hodoscope [13].*

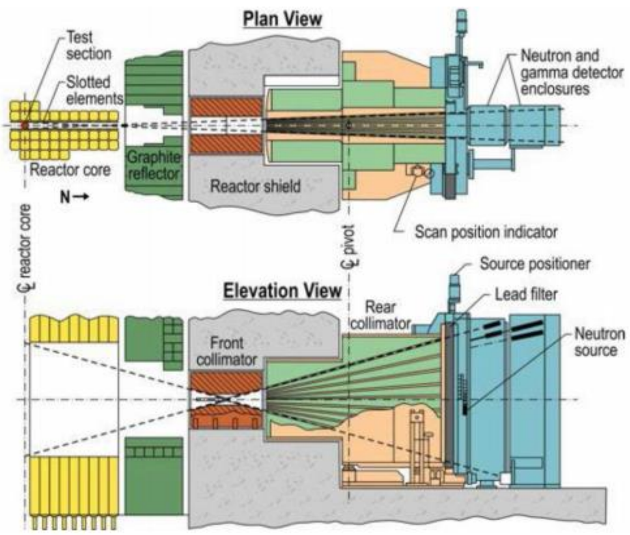

Figure 2. *Sketch of TREAT with Hodoscope (Plan and Elevation Views) [13].*

1.3. Choice of Filters

The paper titled as "Filtered Back-Projection in 4-Pi Compton Imaging with a Single 3D Position Sensitive CdZnTe Detector" by Dan Xu provides image reconstruction algorithms for Compton scattering cameras that provide higher detection efficiency without the use of a mechanical collimator. This paper investigates a filtered back projection algorithm applied to a single 3-dimensional position sensitive CdZnTe detector. This paper concludes that the filtered back projection algorithm performed in spherical harmonics reduces the computation time and cost and because of its linear property; the FBP reconstruction can be performed event-by-event for real time imaging.

The paper titled "Utilization of an optimum low-pass filter during filtered back projection in the reconstruction of single photon emission computed tomography images of small structures" by Mpumelelo Nyathi was used to understand the types of filters and their application in improving the quality of the filtered back projection (FBP) image by eliminating the noise. This study aimed at selection of an optimum low-pass filter for FBP reconstruction of Single Photon Emission Computed Tomography (SPECT) images of small structures. A low pass filter allows the retention of low frequencies while blocking higher frequencies and when used in conjunction with the ramp filter will yield a better image. The Parzen, the Hanning, and the Butterworth filters are among the commonly used low-pass filters [6]. The Parzen filter is a smoothing filter, which can eliminate noise at high frequency. However, it degrades the spatial resolution. The Butterworth filter is a low-pass filter that is generally preferred in SPECT image filtering. It has the potential of reducing the noise while preserving image resolution. It is well suited for utilization due to its ability to change the shape through the cut-off frequency and the order parameter [6]. On the other hand, the ramp filter is a high pass filter that eliminates the star artifact consequences of a simple projection by allowing the passage of high frequencies and restricting the passage of low frequencies.

Several image reconstruction techniques have been used such as maximum likelihood algorithms, and algebraic reconstruction techniques (ART). However, these are indirect methods and are computationally intense [5].

2. Theory

The image of an object is formed by the convolution of the object function (source profile) and the point spread function (PSF) of the imaging system [16]. The PSF of the system is the weighted average over the entire energy spectrum that causes blurring effects of diffraction, pinhole geometry, and the hodoscope detector [14]. PSF gives the degree of blurring caused by diffraction and this function is useful in extracting the right beam size out of the pinhole image. The equation below represents the relationship between object and an image [4].

$$g(x, y) = \iint_{\infty}^{\infty} f(x', y') h(x, x'; y, y') dx' dy' \quad (1)$$

where $g(x, y)$ the two-dimensional image of a two-dimensional object $f(x', y')$, and the function h is the point spread function that tells how information from a point source spreads out over the image plane. If we assume a point source (delta function), the point-spread function has the same form as the image from a point source like the impulse response in 1D. Equation 2 below represents a simple object-image relationship [10].

$$g(x, y) = f(x, y) \otimes\otimes h(x, y) \quad (2)$$

Where, the operator $\otimes\otimes$ is the convolution integral and h(x, y) is the point spread function.

A low pass (e.g., Hann) filter is characterized by the cut off frequency. The cut off frequency or roll-off frequency is defined as the frequency above which the noise is reduced or eliminated. The Hann filter is defined in the frequency domain as: [12]

$$H(f) = \begin{Bmatrix} 0.54 + 0.46 \cos\left\{\frac{\pi f}{f_m}\right\}, 0 \le |f| \le f_m \\ 0 \ otherwise \end{Bmatrix} \quad (3)$$

where f is the spatial frequencies of the image and f_m is the cut-off frequency. It is very effective in reducing the noise since it reaches zero very quickly as seen from the figure 3.

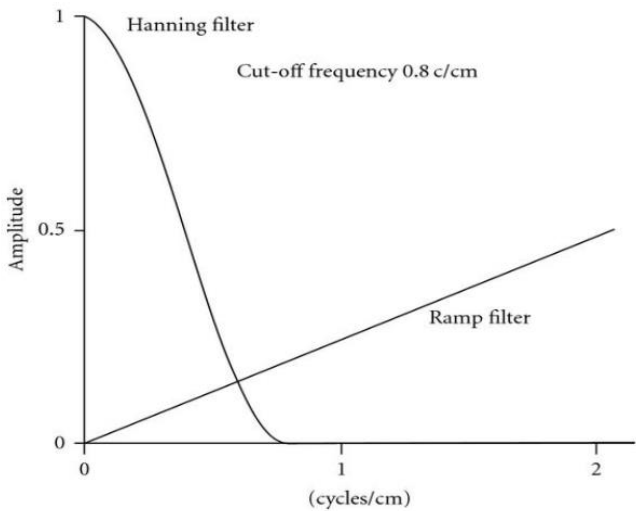

Figure 3. *Different Filters [12].*

3. Materials and Methods

A detailed model of TREAT reactor was built in MCNP with central fuel element replaced by dummy slotted fuel containing the sample [11]. In the MCNP model, k-code was run with flux mesh on the xz axis and the point flux tallies on the locations where we need the fluxes. One of the important point to note is that the model obtained was for a critical system and the source-driven problem does not work since MCNP need to track infinite particles. It needs to be modified to be in a slightly sub-critical state. One more note, MCNP has no concept of time, so we need to define a source and it generates particles and tracks them. Any fluxes we obtain are based on per source particle hence we might notice flux values in decimals.

There are three control rod types. There are four compensation rods located near the center of the core, four pairs of control rods and four pairs of transient rods. Rods are driven from the bottom and are pushed up to add reactivity and dropped down to shut down. Another important point to note is that the transient rods are ejected from the core to produce transient.

4. Results

Figure 4 below shows the corresponding MCNP model with the viewing slot added to provide open path for sample and hodoscope plane [17].

The MCNP calculations were performed in this model. The MCNP input deck is given in the Appendix B. We ran one million histories and used F4 tallies to obtain the flux plot. F4 tally uses track length estimator and scores the number of particle-track lengths per unit volume. The ststistical uncertanities are within the range of 0.015 to 0.02 which fall below 2%.

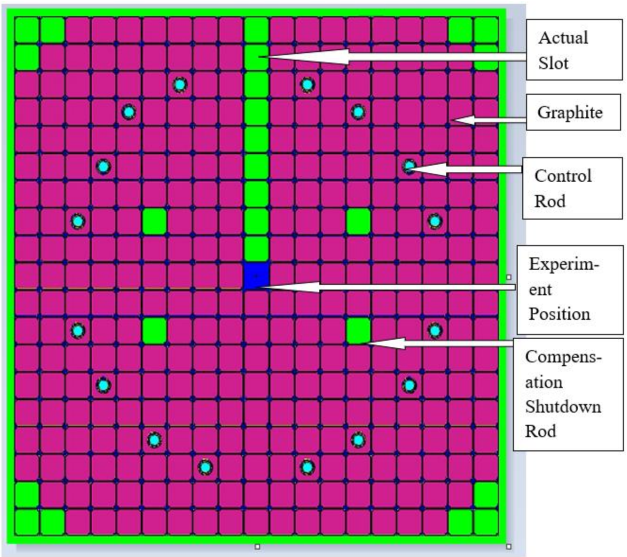

Figure 4. *Plot of TREAT Core X-Y Cross-Section with Slot.*

The point flux tallies, and the mesh tallies were added to determine the flux at different distances from the center to the hodoscope location. It is an eigenvalue calculation but not a fixed source calculation. Flux data at varying distances were imported and plotted first with no fuel in the center. The average and uncollided vertical flux profile at the hodoscope plane (x=hodoscope distance, y=0) are plotted in the following figure 5.

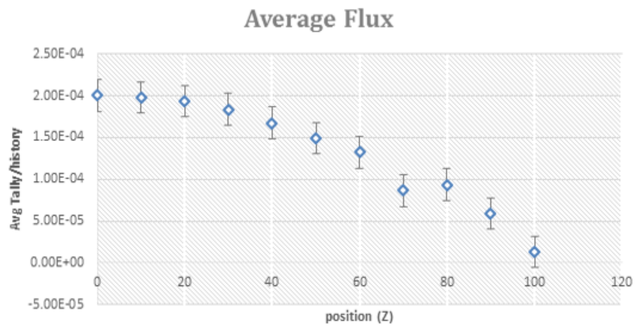

Figure 5. *Average Flux Plot at hodoscope Plane.*

Filtered back projection technique may be applied to the TREAT core imaging with a suitable filter. Figure 6 below shows the reconstruction of the TREAT core with a slotted fuel element for the test capsule without using any filter. TREAT image data were extracted in Mathematica to see if we can reconstruct it with a suitable filter. The flux plots presented were used to make an image. With appropriate radon and inverse radon transformation, following image was reconstructed. Based on the plots, suitable filter will be selected for the future TREAT imaging.

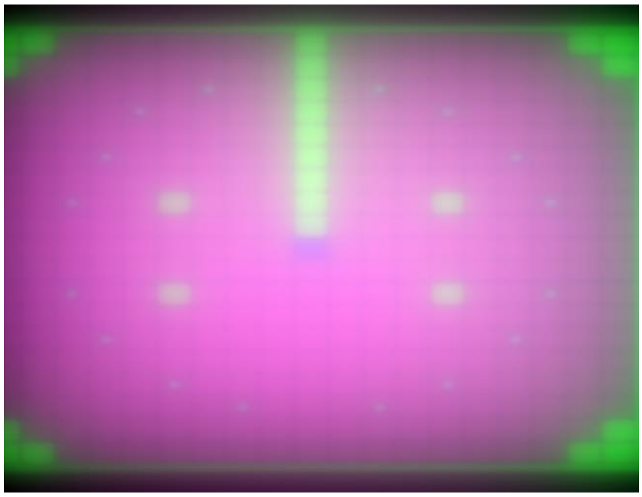

Figure 6. *Reconstruction of TREAT core with No Filter.*

The next step in the process is to include filters to process the image shown in figure 6. Figure 7 below shows the reconstruction of the TREAT core using the FBP technique with a ramp filter. Ramp filter is a high pass filter that filters out the low frequencies and allows the high frequencies. It was found that the ramp filter increased the resolution and quality of the image. However, it still magnifies noise coming from the projection data and it was not the perfect filter. This filter may work reasonably well for images with less complex frequency distribution.

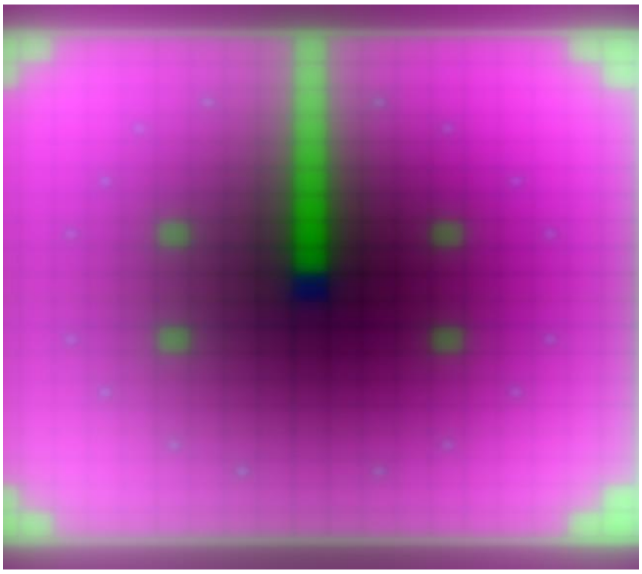

Figure 7. *Reconstruction of TREAT core with Ramp Filter.*

The Hann filter is a low-pass filter (smoothing filter) that filters out the high frequencies and allows the low frequencies. It was found that the Hann filter increased the resolution and quality of the image. FBP technique in conjunction with Hann filter reduces the noise that causes blurring to yield better resolution image as expected. However, it does not preserve edges so suitable cut off frequency need to be selected which will be discussed in the following section.

Figures 8, 9 and 10 below shows the reconstruction image of the TREAT core with slotted fuel element using Hann filter with varying cut-off frequencies as 0.1, 0.3 and 1 cycles/cm respectively.

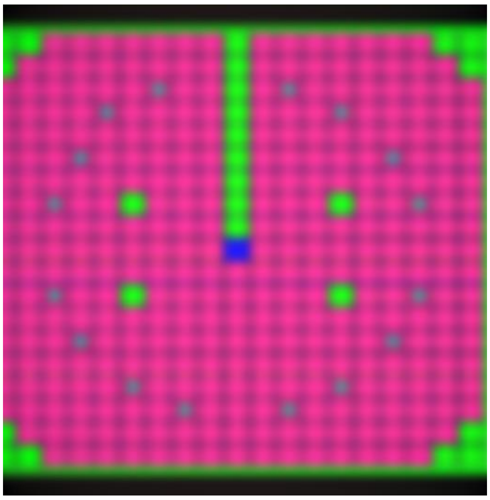

Figure 8. *Reconstruction of TREAT core with Hann Filter, w=0.1.*

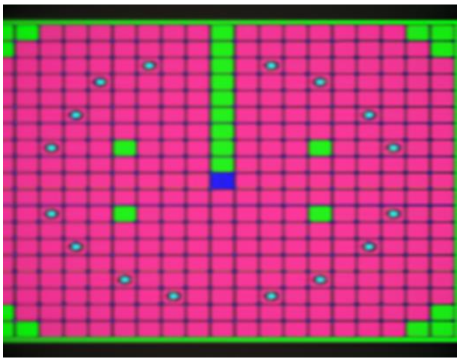

Figure 9. *Reconstruction of TREAT core with Hann Filter, w=0.3.*

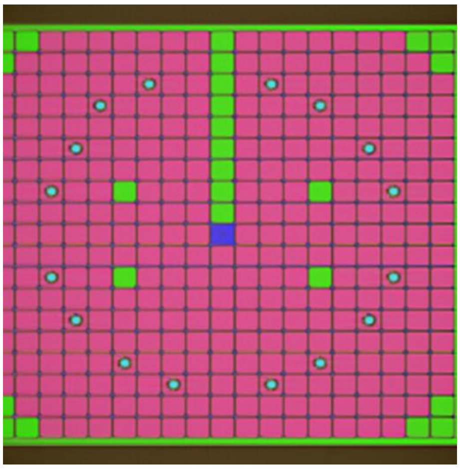

Figure 10. *Reconstruction of TREAT core with Hann Filter, w=1.*

5. Conclusion

This research successfully modeled TREAT using MCNP with a central fuel element replaced by dummy slotted fuel with a sample added to get flux information. Flux information was obtained at the hodoscope plane.

Another avenue of this paper is to support imaging of the test specimen during transient and quantify the mass based on hologram data to understand imaging and with the right choice of filter, we can improve the resolution [15]. Most of the imaging tools use numerical computations, but analytical analysis helps to build insight and this research provides multiple analytical illustrations on using Fourier transform and filtering. A suitable selection of filters is necessary for imaging and the Hann filter works best as shown by multiple examples. In addition to the right choice of filter, the appropriate choice of cut-off frequency removes noises that cause blurring as seen in the previous chapters. It was observed from the figures above that the value of cut-off frequency determines how the filter will affect both image noise and resolution. In other words, the higher the cut-off frequency, the better the spatial resolution, and therefore much more detailed image can be obtained. In conclusion, the Hann filter with a cut-off frequency close to 1 cycle/cm would be recommended for the final image reconstruction.

The imaging techniques described in this paper can be used in nuclear medicine for developing diagnostic and therapeutic modalities. For instance, to treat tumor cells a radioactive drug is typically administered in targeted organs along with gamma cameras to acquire two-dimensional projections of the activity. These projections data are then filtered and back-projected to get the image of the targeted organ. Proper selection of filter and cut-off frequencies are crucial in imaging as discussed in previous sections of the dissertation. Provided more time and support, we will be exploring research in medical applications in the future.

6. Limitations and Future Research

There were a few challenges in completing this research. Some of the shortcomings were: the lack of the most recent TREAT hodoscope data, slight mass discrepancies in data, and the fact that the integrations in analytical solutions were not straightforward in some cases. In those cases, Taylor series expansion was used to find the first 10 coefficients that give convergence in the solution. Some possible reasons for mass discrepancies might be due to self-shielding, data errors, or unknown errors. The mass discrepancy might be more prominent in three pins than that in a single-pin test fuel due to greater chances of self-shielding [18]. This research provides the significance of self-shielding present in the hodoscope data, and it might be a major contributor on mass conservation ambiguities. Had there been single-pin test data available, it would be better if we can relate the trend or better explain the behavior. Nonetheless, this research has several applications in medical imaging and future transient testing.

Author Contributions

Harish Aryal is the sole author. The author read and approved the final manuscript.

Conflicts of Interest

The authors declare no conflicts of interest.

References

[1] Gupta, N. N. Das and Ghosh, S. K. A Report on the Wilson Cloud Chamber and its Applications in Physics. Calcutta, 1946.

[2] Womack, Cody. The Construction and Characterization of a Large Volume Wilson Cloud Chamber Utilizing Orthogonal Cameras for Image Capture" [Thesis].

[3] Wilson, J. G. The Principles of Cloud Chmber Technique, 1951.

[4] Roth, J. and Hobbie, Russel K. Intermediate Physics for Medicine and Biology. Textbook. 5th edition, 2015.

[5] Xu, Dan. Filtered Back-Projection in 4-Pi Compton Imaging with a Single 3D Position Sensitive CdZnTe Detector. IEEE 2006.

[6] Nyathi, Mpumelelo. Utilization of an optimum low-pass filter during filtered back projection in the reconstruction of single photon emission computed tomography images of small structures. Department of Medical Physics, Faculty of Health Sciences, SefakoMakgatho Health Sciences University, Ga-Rankuwa, South Africa 2018.

[7] De Volpi and Freese, C. H. Experimental Results and Improvements in the Fast Neutron Hodoscope.

[8] E. Dickerman. High Power Level Transient Reactor Test (TREAT) Facility Sodium Loop Meltdown Experiment on an Unbonded EBR-II Marl I Fuel Pin.

[9] De Volpi, A. Fast Neutron Hodoscope at TREAT: Methods for Quantitative Determination of Fuel Dispersal" by A. De. Volpi et al.; "Fuel-Motion Diagnostics and Cineradiography.

[10] Abramowitz, M. and Stegu, I. A. Handbook of Mathematical Functions with Formulas, Graphs and Mathematical Tables. National Bureau of Standards Applied Mathematics Series – 55, 10th Printing, 1972.

[11] Pope, Chad. A detailed model of TREAT reactor was built in MCNP. 2016.

[12] Lyra, Maria and Ploussi, Agapi. Filtering in SPECT Image Reconstruction. Volume 2011, Article ID 693795, Published 2011.

[13] Jensen, Colby. Experiment Instrumentation for Transient Testing. Advanced Sensors and Instrumentation. 2016.

[14] James J. Duderstadt, Louis J. Hamilton. Nuclear Reactor Analysis. s. l.: John Wiley & Sons, inc., 1976.

[15] Hetrick, David L. Dynamics of Nuclear Reactors. La Grange Park, Illinois: American Nuclear Society, 1993.

[16] Kreyszig, Erwin. Advanced Engineering Mathmatics. Hoboken, New Jersey: John Wiley & Sons Inc, 2006. ISBN 0471728977.

[17] MCNP, Los Alamos National Laboratory (LANL), 1957. Retrived April 2nd, 2017.

[18] Robert Mowshyoung Wu, Shelf- shielding corrections for the TREAT hodoscope interpretation, 1982.

[19] Wachs, Daniel M. and Bumgrardner. John D. *Restarting the Transient Test (TREAT) Facility Reactor for Nuclear Transient Testing Science*: A Special Issue of Nuclear Technology. Nuclear Technology, 205: 10, iv-v. 2019.

[20] Welch, Alex. *Diffusion Cloud Chamber*. Applied Science Research class spring 2012.